

Original Research Article

Adaptation of Battery Energy Storage System on Under-Frequency Load Shedding Scheme Design

Rajeev Jha¹, Baseem Khan^{2,3*}, Om Prakash Mahela^{3,4}, Elisabeth Caro Montero^{3,5,6}, Yeshitila Hailu Tessema², Dejene Hurissa Boku²

¹ Department of Electrical & Electronics Engineering, Allenhouse Institute of Technology, Kanpur, 208008, India

² Department of Electrical and Computer Engineering, Hawassa University, Hawassa 05, Ethiopia

³ Department of Project Management, Universidad Internacional Iberoamericana, Campeche 24560, Mexico

⁴ Power System Planning Division, Rajasthan Rajya Vidyut Prasaran Nigam Ltd., Jaipur 302005, India

⁵ Universidad Europea del Atlántico, C/Isabel Torres 21, Santander 39011, Spain

⁶ Department of Project Management, Universidade Internacional do Cuanza, Estrada Nacional, Bairro Kaluapanda, Cuito-Bié 250, Angola

ABSTRACT

The reliable operation of power systems is crucial for ensuring uninterrupted power supply to consumers. However, any deficiency in power generation can lead to frequency deviation, disrupting the entire power system. To address this challenge, an active power source with a fast response, such as a Battery Energy Storage System (BESS), can prove to be a highly effective countermeasure. The BESS has gained immense popularity for its diverse applications, including load leveling, frequency and voltage support during loss of generation, improving transient and dynamic stability, and enhancing power quality. This has made the BESS an invaluable contribution to power system restructuring. One of the most important applications of the BESS is in Load Frequency Control, where a proportional-integral (PI) controller is employed to modify the power output of the BESS, resulting in further optimization of the system. In this work, a two-area hydro-thermal interconnected system is considered, and simulations are performed in MATLAB to analyze the impact of the BESS with and without a PI Controller. The results demonstrate a significant reduction in the load shedding amount, and the under-frequency load shedding (UFLS) scheme is made even more effective, ensuring the reliable and uninterrupted operation of the power system.

Keywords: Critical Frequency; Critical Load; Battery Energy Storage System (BESS); Proportional Integral (PI) Controller; Under-Frequency Load Shedding (UFLS)

ARTICLE INFO

Received: Dec 28, 2022

Accepted: Mar 19, 2023

Available online: Mar 31, 2023

*CORRESPONDING AUTHOR

Baseem Khan
baseem.khan04@gmail.com

CITATION

Jha R, Khan B, Mahela OP, *et al.* Adaptation of Battery Energy Storage System on Under-Frequency Load Shedding Scheme Design. Journal of Autonomous Intelligence 2022; 5(2): 44–55.
doi: 10.32629/jai.v5i2.542

1. Introduction

The power system frequency condition depends on the generation-load balance. Under normal operation of the power system, the generation-load balance is maintained, thus the frequency of the power system network remains fixed or deviates within acceptable limits. But, due to a sudden increase in the system load demand or due to a sudden decrease in the generation, the generation-load balance is disturbed and frequency gets deviated from its nominal value. Due to the large generation-load imbalance, the frequency drops beyond its acceptable limit. As there is no direct control on the utility load, to restore system frequency, there is a need of emergency control, i.e., load shedding, if the available power reserve is insufficient to meet the load demand.

The load shedding curtails the amount of load in the power system

COPYRIGHT

Copyright © 2023 by author(s).

Journal of Autonomous Intelligence is published by Frontier Scientific Publishing. This work is licensed under the Creative Commons Attribution-NonCommercial 4.0 International License (CC BY-NC 4.0). <https://creativecommons.org/licenses/by-nc/4.0/>

until the available generation can supply the remaining loads. This must be done with considerate planning as there is no benefit in shedding excessive load. The objective of an effective load shedding scheme is to curtail a minimum amount of load, and provide a quick, smooth, and safe transition of the system from an emergency situation to a normal equilibrium state. Several schemes have been proposed to restore system frequency, post large disturbances. One of these schemes is the use of under frequency load shedding relays^[1-5]. Many authors proposed under-frequency load shedding schemes based on frequency (f). The disadvantage of these schemes was that, it sheds a fixed amount of load irrespective of the disturbance magnitude. Efforts have been made to make the scheme adaptive by considering the rate of change of frequency (df/dt) as an additional control index for effective load shedding^[1-4,6-9].

The power system frequency deviation is a direct consequence of generation deficiency. Hence in order to compensate for this generation deficiency, an active power source with fast response like a Battery Energy Storage System can be a better counter-measure. Energy storage systems like the BESS have proved numerous applications in load leveling, frequency and voltage support during loss of generation, enhancing transient and dynamic stability, improving power quality, and thus proved best contribution in power system restructuring. The BESS is being used for frequency regulation in load frequency control^[10-16].

1.1 Related work

The design of load shading schemes for conventional and hybrid power systems was studied by a number of scholars. The adaptive underfrequency load shedding in systems with renewable energy sources and storage capability was presented in the study by Silva Jr and Assis^[17]. Hongesombut *et al.*^[18] described how they used a fictitious inertia-controlled-battery energy storage system to improve the under frequency protection of an island active distribution network. Eliassi *et al.*^[19] investigated the favoritism and unfairness of the frequency support provided by the grid-interactive battery energy storage system (BESS) in terms of rate of change of frequency (RoCoF), frequency nadir, time response, steady-state error, and specifically, total load shed subject to power balance over the network. The adaptive under-frequency load shedding control technique of power networks using wind turbines and ultra-high voltage DC (UHVDC) to regulate frequency was presented in the study by Wu *et al.*^[20]. The frequency regulation of an off-grid system with a battery energy storage system utilizing a deep Q-network was given in the study of Takayama *et al.*^[21]. The battery energy storage system for load frequency regulation of an interconnected power system was presented by Aditya and Das in their study^[22]. The adaptability in load shedding under risky operating situations was presented by Jung *et al.*^[23]. The new load shedding technique

for limiting underfrequency was presented by Praetijo *et al.*^[24].

1.2 Research gap

Most of the authors adopted the BESS alone to improve the frequency deviation. In this paper, integration of PI and the BESS gives more better results on the shaded amount of the demand as compared with the BESS alone.

1.3 Contribution

This paper explores the impact of integration of PI and the BESS on under-frequency load shedding scheme design. The novel contribution of the paper is as follows.

- 1) The BESS is used to design the under-frequency load shedding scheme.
- 2) A PI Controller is utilized in association with the BESS to minimize the shaded amount of demand.
- 3) A detailed comparative analysis is presented to show the effectiveness of the proposed battery energy storage system integrated with a PI Controller.

2. System configuration

Typically, a two-area system inter-connects two control areas to exchange their power output to meet the demands of each other and hence provide secure, stable and reliable operation of the power system post system disturbance in either of the control areas. A tie line is the means of connecting the control areas to exchange the power of the control areas by modulating the tie line power. In this paper, a two-area thermal-hydro power system model is being considered for load shedding, taking load disturbances in both areas. The impact of the BESS on load shedding is being modeled, simulated and results are compared for load shedding steps considering three cases first without the BESS and second with the BESS (without a PI Controller) and third with the BESS (with a PI Controller) in the thermal area. The BESS produces a power output proportional to the frequency deviation. The PI Controller further regulates the power production, hence the frequency and load shedding amount.

3. Proposed work

3.1 Model without the BESS

The block diagram of a two-area thermal-hydro power system without the BESS is given in **Figure 1**. The change in demand ΔP_d is considered to be a step function. The sign of ΔP_d is such that, for a sudden increase in load demand $\Delta P_d > 0$, for a sudden increase in generation $\Delta P_d < 0$. The step load change is expressed as:

$$\Delta P_d(t) = \Delta P_L u(t) \quad (1)$$

where ΔP_L is the disturbance magnitude in per unit on system volt-ampere base SSB and $u(t)$ is a usually defined step function. In Laplace domain Eq. (2) can be expressed as:

$$\Delta P_d(s) = \frac{\Delta P_L}{s} \quad (2)$$

3.2 Battery Energy Storage System (BESS)

A BESS generally consists of an AC/DC converter, a battery matrix consisting of a set of batteries in series and parallel connection and a control scheme. The control scheme determines the operation of the converter, based on information from the AC side of the converter as well as from the battery matrix^[22]. To get information from the batteries, a battery management system is needed. The system should be designed to maximize the lifetime and reliability of the BESS. This could be achieved by operating the individual strings of the battery matrix based on parameters like voltage, current, temperature, state of charge (SOC) and state of health (SOH) of the batteries.

3.2.1 Mathematical modeling of the BESS

The mathematical modeling of a Battery Energy Storage System can be discussed as follows.

- 1) Transfer function equation of fuel cells

The transfer function of a Battery Energy Storage System (BESS) and a fuel cell are generally different, as they have different physical and chemical characteristics. However, the dynamics of the two systems may be similar enough that similar

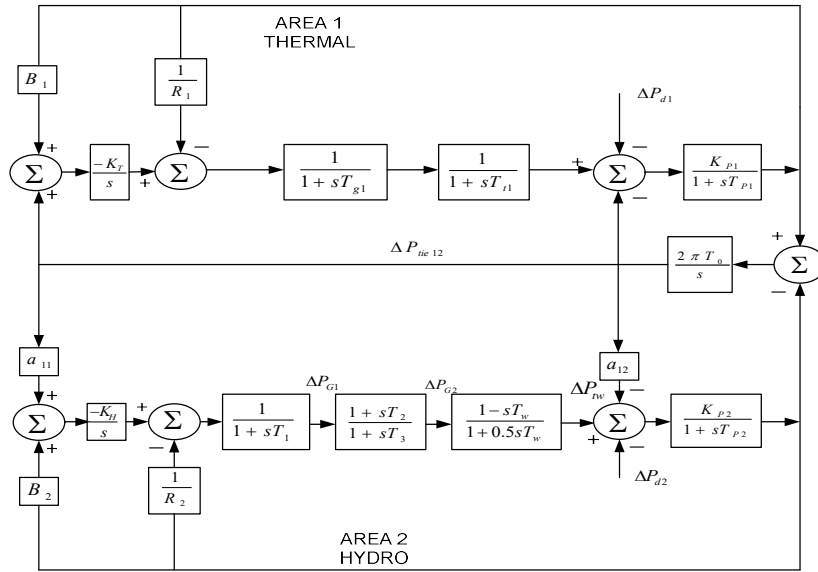


Figure 1. Block diagram of the thermal-hydro system without the BESS.

control strategies can be used. So the authors used the transfer function of fuel cells.

One more assumption taken by the authors to use a first-order transfer function for the system is that it provides a simple and efficient model for the dynamics of the system. First-order transfer functions are commonly used to represent the behavior of systems that have a single dominant time constant, and can be an adequate approximation for some energy storage systems like the BESS. Additionally, using a high-order nonlinear model can increase the complexity of the control algorithm and require more computational resources. A simpler model may be more practical for implementation, especially in real-time applications. However, it's worth noting that the choice of models depends on the level of accuracy required for the control application. If the control application requires high accuracy, a higher-order model may be necessary to capture the nonlinear dynamics of the system.

A number of high-order non-linear BESS models have been proposed in the literature but a rather simple first-order approximated battery model is being used in the work and is characterized by a first-order transfer function as given below:

$$\frac{\Delta P}{\Delta f} = \frac{K_{BESS}}{1 + sT_{BESS}} \quad (3)$$

where,

ΔP = Active output power of the BESS (pu. MW);

Δf = Frequency deviation [(f - 50)/50] (pu. Hz);

K_{BESS} = Gain constant of the BESS (p.u.MW/p.u. Hz);

T_{BESS} = Time constant of the BESS (sec.).

2) Control scheme of the BESS unit

The BESS unit is being controlled by its current state of charge (ΔSOC). Controlling of the BESS unit can be discussed in two modes:

a) Charging mode

The battery state of charge (SOC) in the charging mode can be represented as a transfer function given below:

$$\Delta SOC_{ch} = \frac{\eta_{BESS}}{s * 3600 * W_{BESS}} \quad (4)$$

where,

η_{BESS} = Efficiency of the BESS;

W_{BESS} = Power rating of the BESS.

The battery is charging during off peak load hours and current is being drawn by the battery from the utility grid. It is in the discharging mode during peak load hours and current is being supplied by the battery to the utility grid.

When the current change in battery SOC (ΔSOC) is lower than the upper limit of SOC (SOCU), i.e., the upper charging state, the battery is

in the charging mode. If ΔSOC is greater than SOC_U , then there will be no action state.

2) Discharging mode

The battery state of charge (SOC) in the discharging mode can be represented as a transfer function given below:

$$\Delta SOC_{dch} = \frac{1}{s * 3600 * W_{BESS}} \quad (5)$$

When the current change in state of charge (ΔSOC) is greater than the lower limit of SOC

(SOCL), the battery will be in the discharging mode otherwise no action mode.

3.2.2 Model with the BESS (without a PI Controller)

With the BESS, the block diagram as shown in Figure 2 can be modified and shown in Figure 3. With the BESS in the thermal area, the active power support in the thermal area increases and thus, there is less load shedding amount results.

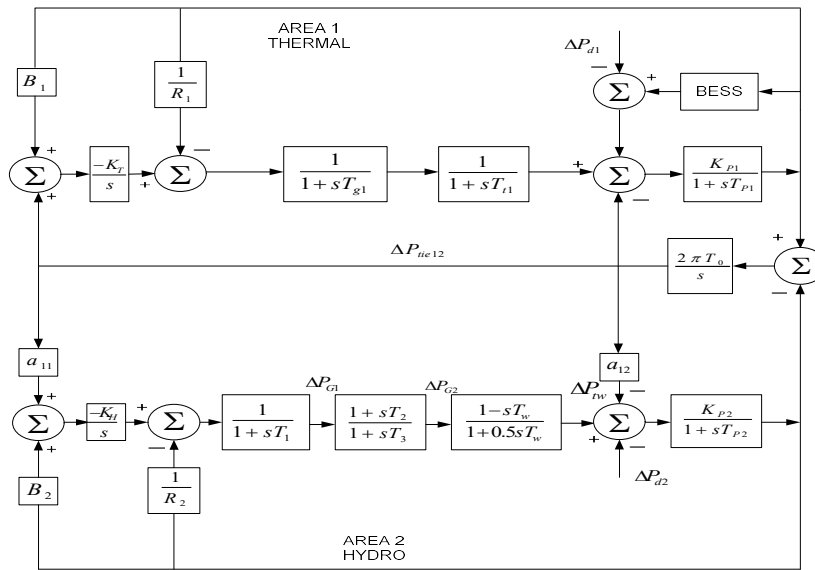


Figure 2. Block diagram of the thermal-hydro power system with the BESS (without a PI Controller).

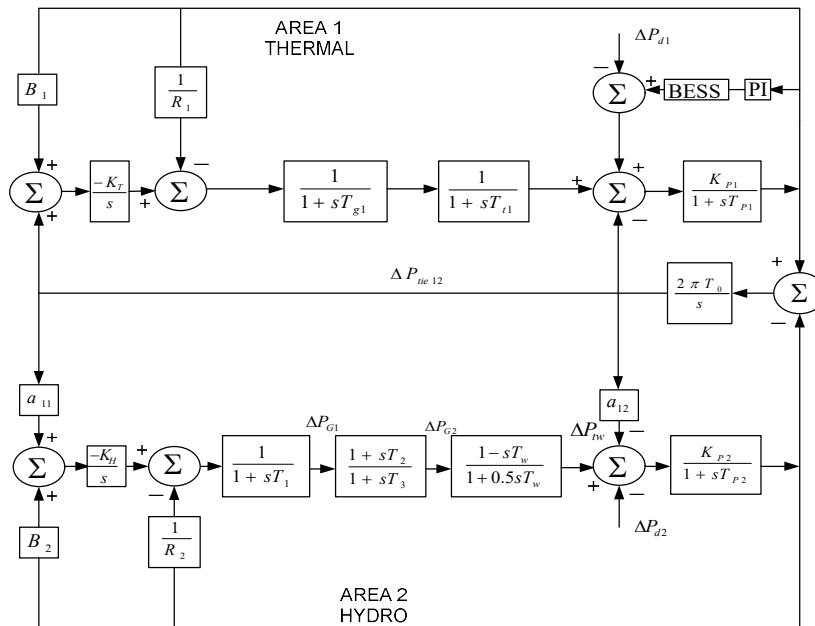


Figure 3. Block diagram of the thermal-hydro system with PI controller based FCS.

3.2.3 Model with the BESS (with a PI Controller)

With the BESS in the thermal area, the block diagram as given in **Figure 2** can be modified and shown in **Figure 3**. In the present section, the PI Controller is included in the BESS.

The different system parameters based on the above discussed models are presented in **Table 1**.

Table 1. System parameters

| S. No. | Parameters | Values |
|--------|------------------|-----------------|
| 1 | K_{P1}, K_{P2} | 120 Hz/(pu. MW) |
| 2 | T_{P1}, T_{P2} | 20 sec. |
| 3 | R_1, R_2 | 2.4 Hz/(pu. MW) |
| 4 | B_1, B_2 | 0.4249 |
| 5 | T_{g1} | 0.08 sec. |
| 6 | T_{t1} | 0.3 sec. |
| 7 | T_0 | 0.0866 sec. |
| 8 | T_1 | 41.6 sec. |
| 9 | T_2 | 5 sec. |
| 10 | T_3 | 0.513 sec. |
| 11 | T_w | 1 sec. |
| 12 | D_1, D_2 | 8.333 pu. MW/Hz |

4. Simulation result and discussion

After simulation of the two-area interconnected thermal-hydro system, three studies were found:

Table 4. Frequency variation of Area 1 and Area 2 with corresponding load shed w.r.t. equally varying load in both areas without the BESS

| Case No. | ΔP_{L1} (pu) | ΔP_{L2} (pu) | Δf_{1max} (Hz) | Δf_{1min} (Hz) | Δf_{2max} (Hz) | f_{2min} (Hz) | LSA ₁ (pu) | LSA ₂ (pu) |
|----------|----------------------|----------------------|------------------------|------------------------|------------------------|-----------------|-----------------------|-----------------------|
| 1 | 0.2 | 0.2 | -1.03 | 48.97 | -1.29 | 48.71 | NA | NA |
| 2 | 0.3105 | 0.3105 | -1.59 | 48.41 | -2 | 48 | NA | NA |
| 3 | 0.3921 | 0.3921 | -2 | 48 | -2.5 | 47.5 | NA | 0.0816 |
| 4 | 0.45 | 0.45 | -2.31 | 47.69 | -2.9 | 47.1 | 0.0579 | 0.1395 |
| 5 | 0.5 | 0.5 | -2.58 | 47.42 | -3.2 | 46.8 | 0.1079 | 0.1895 |
| 6 | 0.6 | 0.6 | -3.08 | 46.92 | -3.86 | 46.14 | 0.2079 | 0.2895 |
| 7 | 0.645 | 0.645 | -3.3 | 46.7 | -4.1 | 45.9 | 0.2529 | 0.3345 |
| 8 | 0.8 | 0.8 | -4.1 | 45.9 | -5.15 | 44.85 | 0.4079 | 0.4895 |
| 9 | 1 | 1 | -5.1 | 44.9 | -6.4 | 43.6 | 0.6079 | 0.6895 |

first without the BESS, second with the inclusion of the BESS without a PI Controller and third with a PI controller. All studies were simulated in the time domain using MATALAB/Simulink Software and compared the result of three scenarios. Some time constants considered in this work for better finding results are presented in **Table 2**. Out of these four BESS time constant values, authors got the adequate results for $T_{BESS} = 0.05$. Further, **Table 3** presented the FCS parameters and controller gains.

Table 2. Different FC time constants (TFC)

| S. No. | Constant value |
|--------|----------------|
| 1 | 0.04 |
| 2 | 0.05 |
| 3 | 0.06 |
| 4 | 0.07 |

Table 3. FCS parameters and controller Gains

| S. No. | Constant/gain | Value |
|--------|--|-------|
| 1 | Gain Constant of the BESS (K) | 1,000 |
| 2 | Time Constant of the BESS (T_{BESS}) | 0.05 |
| 5 | Proportional Gain of the BESS | 5 |
| 6 | Integral Gain of the BESS | 10 |

4.1 Scenario 1: Effect of change in load without the BESS facility

Following observations can be drawn from **Table 4**.

- 1) The critical load for Area 1 (thermal area) is 0.3921 pu, while for Area 2 (hydro area), it is found to be 0.3105 pu. Thus, the critical load for Area 2 is lower than that for Area 1.
- 2) For Area 1, Cases 1–3, no load shedding as up to the critical load is required. But as the load increases beyond the critical load, the frequency decreases below its minimum allowable frequency, i.e., critical frequency.
- 3) For Area 2, Cases 1–2, no load shedding as up to the critical load is required. But as the load increases beyond the critical load, the frequency decreases below its minimum allowable frequency, i.e., critical frequency.
- 4) Load shedding steps for Area 2 (hydro area) is more than that for Area 1 (thermal area).

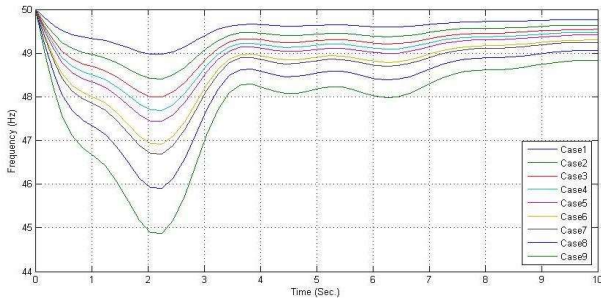


Figure 4. Frequency response of Area 1 without the BESS.

From **Figure 4**, it shows that for Area 1, the maximum change in frequency is computed and found to be $\Delta f_{1\max} = -5.1 \Delta P_L$ and time instant of maximum frequency change is found to be $t_{1m} = 2.21$ s.

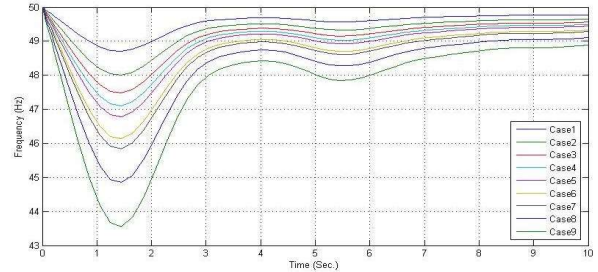


Figure 5. Frequency response of Area 2 without the BESS.

From **Figure 5**, it shows that for Area 2, the maximum change in frequency is computed and found to be $\Delta f_{1\max} = -6.4 \Delta P_L$ and time instant of maximum frequency change is found to be $t_{1m} = 1.40$ s.

4.2 Scenario 2: Effect of change in load with the BESS facility (without a PI controller)

The effect of change in load with the BESS facility without using a PI controller is defined in **Table 5**.

Table 5. Frequency variation of Area 1 and Area 2 with corresponding load shed w.r.t equally varying load in both areas with the BESS (without a PI Controller)

| Case No. | ΔP_{L1} (pu) | ΔP_{L2} (pu) | $\Delta f_{1\max}$ (Hz) | $\Delta f_{1\min}$ (Hz) | $\Delta f_{2\max}$ (Hz) | $f_{2\min}$ (Hz) | LSA ₁ (pu) | LSA ₂ (pu) |
|----------|----------------------|----------------------|-------------------------|-------------------------|-------------------------|------------------|-----------------------|-----------------------|
| 1 | 0.2 | 0.2 | -0.62 | 49.38 | -0.8 | 49.2 | NA | NA |
| 2 | 0.3105 | 0.3105 | -0.96 | 49.04 | -1.25 | 48.75 | NA | NA |
| 3 | 0.3921 | 0.3921 | -1.22 | 48.78 | -1.58 | 48.42 | NA | NA |
| 4 | 0.45 | 0.45 | -1.4 | 48.6 | -1.8 | 48.2 | NA | NA |
| 5 | 0.5 | 0.5 | -1.55 | 48.45 | -2 | 48 | NA | NA |
| 6 | 0.6 | 0.6 | -1.86 | 48.14 | -2.4 | 47.6 | NA | 0.1 |
| 7 | 0.645 | 0.645 | -2 | 48 | -2.6 | 47.4 | NA | 0.145 |
| 8 | 0.8 | 0.8 | -2.5 | 47.5 | -3.22 | 46.78 | 0.155 | 0.3 |
| 9 | 1 | 1 | -3.1 | 46.9 | -4 | 46 | 0.355 | 0.5 |

Following observations can be drawn from **Table 5**.

- 1) The critical load for Area 1 (thermal area) is 0.645 pu, while for Area 2 (hydro area), it is found to be 0.50 pu. The critical load for Area 2 is lower than that for Area 1. Hence the load ability of both the areas increases with the introduction of the BESS facility in the thermal area. With the BESS, the load ability of Area 1 is more than that of the Area 2; this is because of the additional active power support of the BESS facility.
- 2) With BESS support, less load shedding steps are required for both areas. But the load shedding steps are less in Area 1 in which the BESS facility is being provided.
- 3) Load shedding steps for Area 2(hydro area) is more than that for Area 1 (thermal area).

Above-mentioned observations can also be verified from **Figures 6 and 7**.

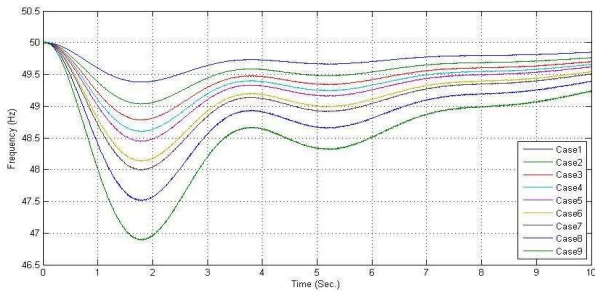


Figure 6. Frequency response of Area 1 with the BESS in the thermal area.

Figure 6 shows that for Area 1, the maximum change in frequency is computed and found to be $\Delta f_{1\max} = -3.1 \Delta P_L$ and time instant of maximum frequency change is found to be $t_{1m} = 1.8$ s.

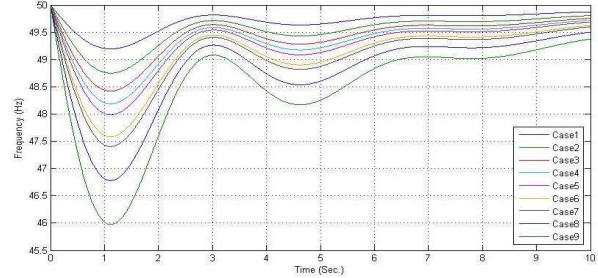


Figure 7. Frequency response of Area 2 with the BESS in the thermal area.

Figure 7 shows that for Area 2, the maximum change in frequency is computed and found to be $\Delta f_{2\max} = -4.0 \Delta P_L$ and time instant of maximum frequency change is found to be $t_{2m} = 1.2$ s.

4.3 Scenario 3: Effect of change in load with the BESS facility (with a PI Controller)

In the scenario 3, effect of the change in the load, with the BESS and a PI Controller is presented. In this work, a PI controller is tuned as per the trial and error method.

Following observations can be drawn from **Table 6**.

- 1) The critical load for Area 1 (thermal area) is 0.9523 pu, while for Area 2 (hydro area), it is

Table 6. Frequency variation of Area 1 and Area 2 with corresponding load shed w.r.t equally varying load in both areas with the BESS (with a PI Controller)

| Case No. | ΔP_{L1} (pu) | ΔP_{L2} (pu) | $\Delta f_{1\max}$ (Hz) | $\Delta f_{1\min}$ (Hz) | $\Delta f_{2\max}$ (Hz) | $\Delta f_{2\min}$ (Hz) | LSA1 (pu) | LSA2 (pu) |
|----------|----------------------|----------------------|-------------------------|-------------------------|-------------------------|-------------------------|-----------|-----------|
| 1 | 0.2 | 0.2 | -0.43 | 49.57 | -0.7 | 49.3 | NA | NA |
| 2 | 0.3105 | 0.3105 | -0.66 | 49.34 | -1.15 | 48.85 | NA | NA |
| 3 | 0.3921 | 0.3921 | -0.84 | 49.16 | -1.46 | 48.54 | NA | NA |
| 4 | 0.5434 | 0.5434 | -1.16 | 48.84 | -2 | 48 | NA | NA |
| 5 | 0.6 | 0.6 | -1.3 | 48.7 | -2.2 | 47.8 | NA | 0.0566 |
| 6 | 0.645 | 0.645 | -1.4 | 48.6 | -2.4 | 47.6 | NA | 0.1016 |
| 7 | 0.8 | 0.8 | -1.7 | 48.3 | -2.95 | 47.05 | NA | 0.2566 |
| 8 | 0.9523 | 0.9523 | -2 | 48 | -3.5 | 46.5 | NA | 0.4089 |
| 9 | 1 | 1 | -2.1 | 47.9 | -3.7 | 46.3 | 0.0477 | 0.4566 |

found to be 0.5434 pu. The critical load for Area 2 is lower than that for Area 1. It can also be seen that in comparison to the above cases, i.e., with only the BESS and with the PI Controller based BESS, the critical load for the present case is much higher. Hence the load ability of both the areas increases with the introduction of the BESS facility in one of the areas (thermal area for the present case). With BESS support in the thermal area (Area 1), the load ability of Area 1 is more than that of Area 2; this is because of the additional active power support of the BESS facility.

2) With BESS support, less load shedding steps are required for both areas in comparison to the above discussed cases. But the load shedding steps are less in Area 1 in which the BESS facility is being provided.

It can be observed from **Figure 8**, that the minimum frequency for Area 1 and Area 2 is higher for the present case in comparison to the above discussed cases; this is only because of the addition power provided by the BESS facility whose power is being further modulated and increased with a PI Controller for better frequency response and hence there is less load shedding amount result. This feature makes the load shedding scheme much more attractive.

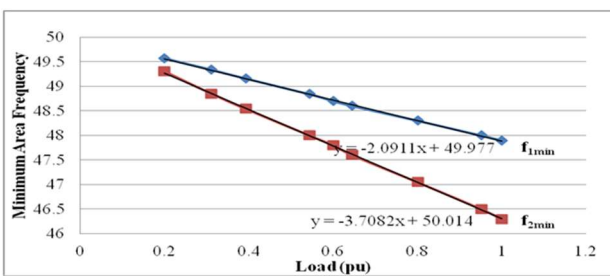


Figure 8. Variation of minimum frequency w.r.t equally varying loads in both areas.

Figure 9 shows that for Area 1, the maximum change in frequency is computed and found to be $\Delta f_{1max} = -2.1 \Delta P_L$ and time instant of maximum frequency change is found to be $t_{1m} = 1.8$ s.

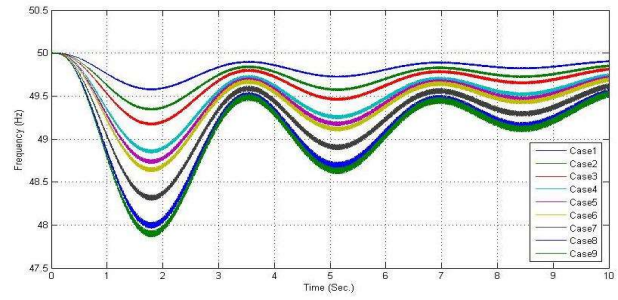


Figure 9. Frequency response of Area 1 with the BESS (with a PI Controller) in the thermal area.

Figure 10 shows that for Area 2, the maximum change in frequency is computed and found to be $\Delta f_{2max} = -3.7 \Delta P_L$ and time instant of maximum frequency change is found to be $t_{1m} = 1.0$ s.

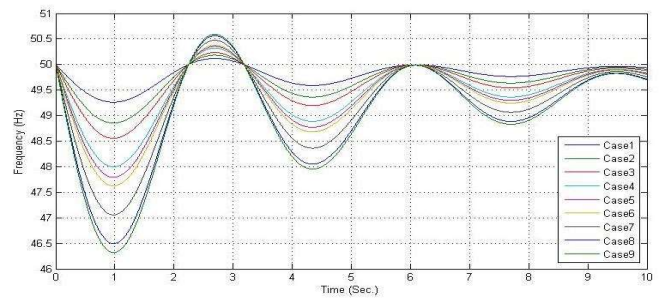


Figure 10. Frequency response of Area 2 with the BESS (with a PI Controller) in the thermal area.

4.4 Comparative analysis

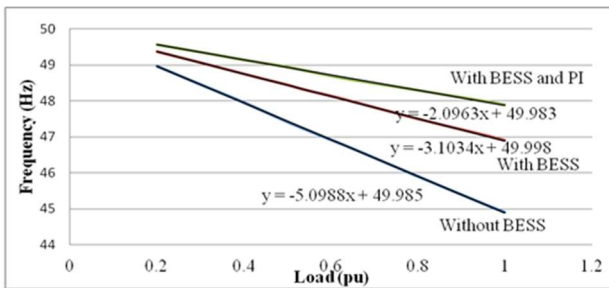
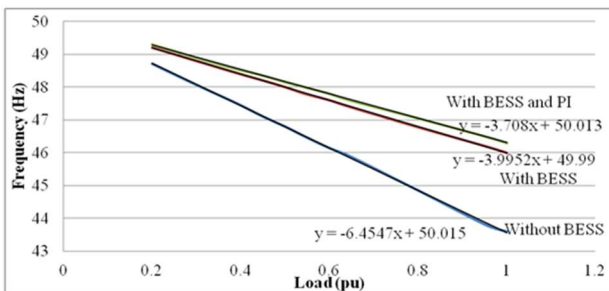
Figures 11 and 12 verify the results given in **Table 7**. It compares the frequency response of the two areas for the different case study schemes. It shows that the schemes incorporating the BESS with a PI Controller show best results among the three discussed cases or schemes. This is only because of the modulation of the BESS power output with the introduction of a PI Controller.

5. Conclusion

Energy storage systems are able to provide value added benefits to improve stability, power quality and security of supply. Energy storage systems have shown and proved their potential applications in load leveling, frequency support (spinning reserve) during loss of generation, enhancing transient and dynamic stability, dynamic voltage support (VAR compensation), improving power quality,

Table 7. Variation of minimum frequencies of both areas without the BESS, with the BESS (without a PI Controller) and with the BESS (with a PI Controller)

| S. No. | Load (pu) | Without the BESS | | With the BESS | | With the BESS and a PI Controller | |
|--------|-----------|------------------|-------------|---------------|-------------|-----------------------------------|-------------|
| | | $\Delta f1$ | $\Delta f2$ | $\Delta f1$ | $\Delta f2$ | $\Delta f1$ | $\Delta f2$ |
| 1 | 0.2 | 48.97 | 48.71 | 49.38 | 49.2 | 49.57 | 49.3 |
| 2 | 0.3105 | 48.41 | 48 | 49.04 | 48.75 | 49.34 | 48.85 |
| 3 | 0.3921 | 48 | 47.5 | 48.78 | 48.42 | 49.16 | 48.54 |
| 4 | 0.45 | 47.69 | 47.1 | 48.6 | 48.2 | 49.05 | 48.35 |
| 5 | 0.5 | 47.42 | 46.8 | 48.45 | 48 | 48.95 | 48.15 |
| 6 | 0.5434 | 47.2 | 46.5 | 48.3 | 47.8 | 48.84 | 48 |
| 7 | 0.6 | 46.92 | 46.14 | 48.14 | 47.6 | 48.7 | 47.8 |
| 8 | 0.645 | 46.7 | 45.9 | 48 | 47.4 | 48.6 | 47.6 |
| 9 | 0.8 | 45.9 | 44.85 | 47.5 | 46.78 | 48.3 | 47.05 |
| 10 | 0.9523 | 45.13 | 43.8 | 47.05 | 46.2 | 48 | 46.5 |
| 11 | 1 | 44.9 | 43.6 | 46.9 | 46 | 47.9 | 46.3 |

**Figure 11.** Frequency variation of Area 1 with different schemes.**Figure 12.** Frequency variation of Area 2 with different schemes.

increasing transmission line capacity, thus enhancing overall security and reliability of power systems. Battery storage systems provide economic benefits of energy storage systems. Due to their low power capacity, they are restricted to be used for small disturbance like load increment in some area and are

not suitable to be used for large generation loss.

Conflict of interest

The authors declared no conflict of interest.

References

- Huang SJ, Huang CC. An adaptive load shedding method with time-based design for isolated power systems. *Electric Power Energy Systems* 2000; 22(1): 51-58. doi: 10.1016/S0142-0615(99)00035-6.
- Terzija VV. Adaptive underfrequency load shedding based on the magnitude of the disturbance estimation. *IEEE Transactions on Power Systems* 2006; 21(3): 1260-1266. doi: 10.1109/TPWRS.2006.879315.
- You H, Vittal V. Self-healing in power systems: An approach using islanding and rate of frequency decline-based load shedding. *IEEE Transactions on Power Systems* 2003; 18(1): 174-181. doi: 10.1109/TPWRS.2002.807111.
- Anderson PM. *Power system protection*. New York, NY: IEEE/Wiley; 1999.
- Shih LJ, Lee WJ, Gu JC, Moon YH. Application of df/dt in power system protection and its implementation in microcontroller based intelligent load shedding relay. In: *Proceedings of Industrial and Commercial Power System Technical Conference*; 1991

- May 6-9; Memphis, TN, USA. IEEE; 2001. pp. 11-17. doi: 10.1109/ICPS.1991.153060.
6. Thompson JG, Fox B. Adaptive load shedding for isolated power systems. IEEE Proceedings-Generation, Transmission, and Distribution 1994; 141(5): 492-496. doi: 10.1049/ip-gtd:19941370.
 7. Anderson PM, Mirheydar M. An adaptive method for setting under-frequency load shedding relays. IEEE Transactions on Power Systems 1992; 7(2): 647-655. doi: 10.1109/59.141770.
 8. Bevrani H, Ledwich G, Ford JJ. On the use of df/dt in power system emergency control. In: Proceedings of IEEE Power Systems Conferences and Exposition (CD Record); 2009 Mar 15-18; Seattle, Washington, USA. IEEE; 2009. doi: 10.1109/PSCE.2009.4840173.
 9. Chuvychin VN, Gurov NS, Venkata SS, Brown RE. An adaptive approach to load shedding and spinning reserve control during under-frequency conditions. IEEE Transactions on Power Systems 1996; 11(4): 1805-1810. doi: 10.1109/59.544646.
 10. Rudez U, Mihalic R. Monitoring the first frequency derivative to improve adaptive under frequency load-shedding schemes. IEEE Transactions on Power Systems 2011; 26(2): 839-846. doi: 10.1109/TPWRS.2010.2059715.
 11. Seyedi H, Sanaye-Prasad M. New centralized adaptive load shedding algorithms to mitigate power system blackouts. IET Generation, Transmission & Distribution 2009; 3(1): 99-114. doi: 10.1049/iet-gtd:20080210.
 12. Kottick D, Blau M, Edelstein D. Battery energy storage for frequency regulation in an island power system. IEEE Transactions on Energy Conversion 1993; 8(3): 455-459. doi: 10.1109/60.257059.
 13. Mercier P, Cherkaoui R, Oudaloe A. Optimizing a battery energy storage system for frequency control application in an isolated power system. IEEE Transactions on Power Systems 2009; 24(3): 1469-1477. doi: 10.1109/TPWRS.2009.2022997.
 14. Kunisch HJ, Kramer KG, Dominik H. Battery energy storage, another option for load frequency control, and instantaneous reserve. IEEE Transactions on Energy Conversions 1986; 1(3): 41-46. doi: 10.1109/TEC.1986.4765732.
 15. Lu CF, Liu CC, Wu CJ. Effect of battery energy storage system on load frequency control considering governor dead band and generation rate constraint. IEEE Transactions on Energy Conversion 1995; 10(3): 555-561. doi: 10.1109/60.464882.
 16. Aditya SK, Das D. Application of battery energy storage system to load frequency control of an isolated power system. International Journal of Energy Research 1999; 23: 247-258. doi: 10.1002/(SICI)1099-114X(19990310)23:3<247::AID-ER480>3.0.CO;2-T.
 17. Silva Jr SS, Assis TML, Adaptive underfrequency load shedding in systems with renewable energy sources and storage capability. Electric Power Systems Research 2020; 189: 106747. doi: 10.1016/j.epsr.2020.106747.
 18. Hongesombut K, Punyakunlaset S, Romphochai S. Under frequency protection enhancement of an islanded active distribution network using a virtual inertia-controlled-battery energy storage system. Sustainability 2021; 13(2): 484. doi: 10.3390/su13020484.
 19. Eliassi M, Torkzadeh R, Mazidi P, *et al.* Conflict of interests between SPC-based BESS and UFLS scheme frequency responses. In: Németh B, Ekonomou L (editors). Flexitranstore. ISH 2019. Lecture Notes in Electrical Engineering, vol 610. Cham: Springer; 2020. doi: 10.1007/978-3-030-37818-9_6.
 20. Wu X, Xue F, Dai J, Tang Y. Adaptive under-frequency load shedding control strategy of power systems with wind turbines and UHVDC participating in frequency regulation. Frontiers in Energy Research 2022; 10: 875785. doi: 10.3389/fenrg.2022.875785.
 21. Takayama S, Sawabe T, Ishigame A, *et al.* Frequency regulation of off-grid system with battery energy storage system using deep Q-network. The Journal of Engineering 2023; 2023(1): e12205. doi: 10.1049/tje2.12205.
 22. Aditya SK, Das D. Battery energy storage system for load frequency control of an interconnected power system. Electric Power Systems Research 2001; 58(3): 179-185. doi: 10.1016/S0378-7796(01)00129-8.
 23. Jung J, Liu CC, Tanimoto SL, Vittal V. Adaptation in

load shedding under vulnerable operating conditions. IEEE Transactions on Power Systems 2002; 17(4): 1199–1205. doi: 10.1109/TPWRS.2002.805023.

shedding scheme for limiting underfrequency. IEEE Transactions on Power Systems 1994; 9(3): 1371–1378. doi: 10.1109/59.336128.

24. Prasetijo D, Lachs WR, Sutanto D. A new load